LA-UR-15-27348
Approved for public release; distribution is unlimited.

Title: Viability of thin wall tube forming of ATF FeCrAl

Author(s): Maloy, Stuart Andrew
Aydogan, Eda
Anderoglu, Osman
Lavender, Curt
Yamamoto, Yukinori

Intended for: Report

Issued: 2016-09-16 (rev.1)

Viability of thin wall tube forming of ATF FeCrAl

Fuel Cycle Research & Development

Prepared for
U.S. Department of Energy
Advanced Fuels Campaign

Stuart A. Maloy, Eda Aydogan, O. Anderoglu, Los Alamos National Laboratory
Curt Lavender, Pacific Northwest National Laboratory
Yukinori Yamamoto, Oak Ridge National Laboratory
Century Tubing, San Diego CA
Rhenium Alloys, Elyria, OH
Sandvik Special Metals Kennewick, WA
LA-UR-

SUMMARY

Fabrication of thin walled tubing of FeCrAl alloys is critical to its success as a candidate enhanced accident tolerant fuel cladding material. Alloys that are being investigated are Generation I and Generation II FeCrAl alloys produced at ORNL and an ODS FeCrAl alloy, MA-956 produced by Special Metals. Gen I and Gen II FeCrAl alloys were provided by ORNL and MA-956 was provided by LANL (initially produced by Special Metals). Three tube development efforts were undertaken. ORNL led the FeCrAl Gen I and Gen II alloy development and tube processing studies through drawing tubes at Rhenium Corporation. LANL received alloys from ORNL and led tube processing studies through drawing tubes at Century Tubing. PNNL led the development of tube processing studies on MA-956 through pilger processing working with Sandvik Corporation. A summary of the recent progress on tube development is provided in the following report and a separate ORNL report: ORNL/TM-2015/478, "Development and Quality Assessments of Commercial Heat Production of ATF FeCrAl Tubes"

THIS PAGE INTENTIONALLY LEFT BLANK

CONTENTS

1.0 Introduction

This report provides a summary of recent results on tube development and characterization performed on FeCrAl alloys. Gen I and Gen II FeCrAl alloys were provided by ORNL and MA-956 was provided by LANL. Three tube development efforts were undertaken. ORNL led the FeCrAl Gen I and Gen II alloy development and tube processing studies through drawing tubes at Rhenium Corporation. LANL received alloys from ORNL and led tube processing studies through drawing tubes at Century Tubing. PNNL led the development of tube processing studies on MA-956 through pilger processing working with Sandvik Corporation. The summary of Gen I and Gen II FeCrAl alloy development and tube processing at Rhenium is provided in ORNL/TM-2015/478, "Development and Quality Assessments of Commercial Heat Production of ATF FeCrAl Tubes". A summary of the tube processing and characterization and testing performed at LANL on Gen I and Gen II FeCrAl alloys is provided in sections 2 and 3. Finally, a summary of the tube processing eventually through pilgering performed at PNNL working with Sandvik on MA 956 is provided in sections 4 and 5.

2.0 Characterization and Testing of FeCrAl Alloys

2.1 **Materials**

The ORNL improved accident tolerant FeCrAl alloys ORNL A and ORNL B (T34 and T54, respectively) were cast by arc-melting in a back-filled argon gas atmosphere, pre-alloyed with Y, Cr and Al. After initial warming at 200 °C followed by annealing at 815 °C for 15 mins, they were drawn at room temperature in sixteen steps. In order to give some stress relief for the further deformation, 15 mins of annealing at 850 °C was applied between each drawing step. After the final drawing step, one of each type was saved to see the effect of cold deformation on the microstructure while the others were exposed to 15 mins of annealing at 850 °C. The samples that did not go through final annealing step were called as 'as-drawn' while the annealed samples after the last deformation step are called as 'annealed'. Final wall thickness of these tubes is ~400 μm with the outer diameter of ~9 mm as shown in Figure 1. Different than first generation alloys, second generation FeCrAl alloy, ORNL Gen II (C35MN6A2), contains Mo, Si and Nb which are very effective in increasing its strength. The alloy was extruded at 800°C, and then annealed at 1200°C for re-solutionization purpose. The nominal chemical compositions are given in wt% in Table 1. Further details of the production steps can be found elsewhere [3].

Figure 1: ORNL A and B first generation alloys.

Table 1: Nominal and analyzed alloy compositions of ORNL nuclear-grade FeCrAl alloys

Alloy	**Fe**	**Cr**	**Al**	**Y**	**Mo**	**Si**	**Nb**	**C**	**S**	**O**	**N**
ORNL A T35	Bal.	13	4.5	.15	-	-	-	N/A	N/A	N/A	N/A
ORNL B T54	Bal.	15	4	.15	-	-	-	N/A	N/A	N/A	N/A
ORNL PII	Bal.	13	5.11	.044	1.99	.18	.96	.005	.0003	.0014	.0002
MA956*	Bal.	19.4	4.21	0.85	-	N/A	-	.02	.007	N/A	N/A

*Also contains 0.42Ti 0.1Mn .074Cu 0.057Ni 0.024Co

Figure 2 Photo showing 10 feet of FeCrAl tubing produced by Century Tubing from Gen I FeCrAl alloys.

2.2 Microscopy

Phase, grain size and orientation distributions resulting from the tube processing were investigated by optical microscopy and EBSD methods. For the phase identification and grain size distribution, optical microscopy was applied in the cross-sectional and longitudinal directions of the first generation ORNL-A and ORNL-B annealed tubes. The samples were metallographically prepared by grinding starting from P800 grit up to P4000 grit followed by polishing with 0.04μm colloidal silica. Then, they were etched by 20ml water-30ml HCl-10ml HNO_3 solution for 2 mins and investigated under optical microscope. On the other hand, the samples examined by EBSD were cut into 3mm TEM foils in the direction as shown in Figure 2. After conventional metallographic preparation steps, they were electropolished with 5 vol% perchloric acid-95 vol% methanol solution at -40 °C with a voltage of 17 V. EBSD scans were

conducted using a FEI Inspect FEG scanning electron microscope (SEM) with TSL EBSD equipment. Since the sample is tilted 70° from the horizontal, diffraction data comes from a very thin surface layer meaning that the results are very surface sensitive. During scans, the acceleration voltage of 20 kV and aperture size of 50 µm was used. The size of the scan region was determined according to the grain size. While the scans are done on a 375µmx1150µm area for the first generation tubular ORNL alloys, 1640µm x 1800 µm region was selected for the second generation alloy. Steps size showing the scan rate of the selected region was kept 1 µm for all scans.

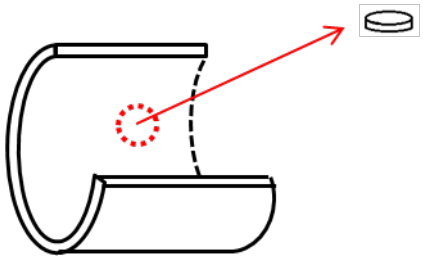

Figure 2: Schematic illustration of the position of TEM foils prepared for EBSD analyses.

2.3 Tensile Tests

Miniature (S1) tensile samples were cut both from tubes of Gen I and bulk Gen II alloy using EDM. The tests were performed at a strain rate of 0.0005 s^{-1} on an Instron 1125. Compliance was corrected using loading slope. Figure 3 shows the miniature tensile test sample schematic. A minimum of two samples of each alloy were tested. High temperature tests were performed under vacuum.

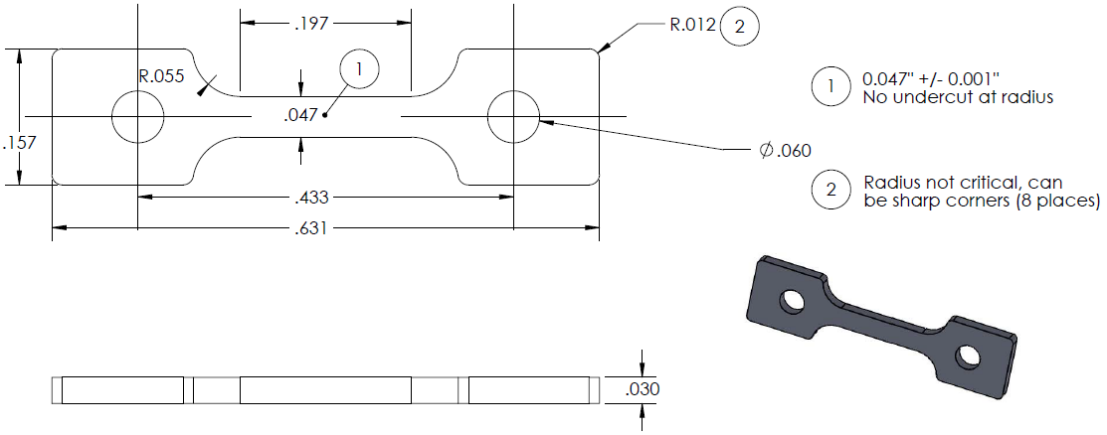

Fig.3. Schematic of miniature tension test samples with dimensions. The samples were cut using EDM.

3. Results and Discussion

3.1.**Characterization**

1st generation ORNL-A and ORNL-B alloys: First generation alloys which are produced in thin walled tubular form consist of uniformly distributed large grains both in longitudinal and cross-sectional directions as shown in Figure 4. It should be also noted that the microstructure consists of large precipitates distributed homogenously among the microstructure and some of them are elongated in the drawing direction.

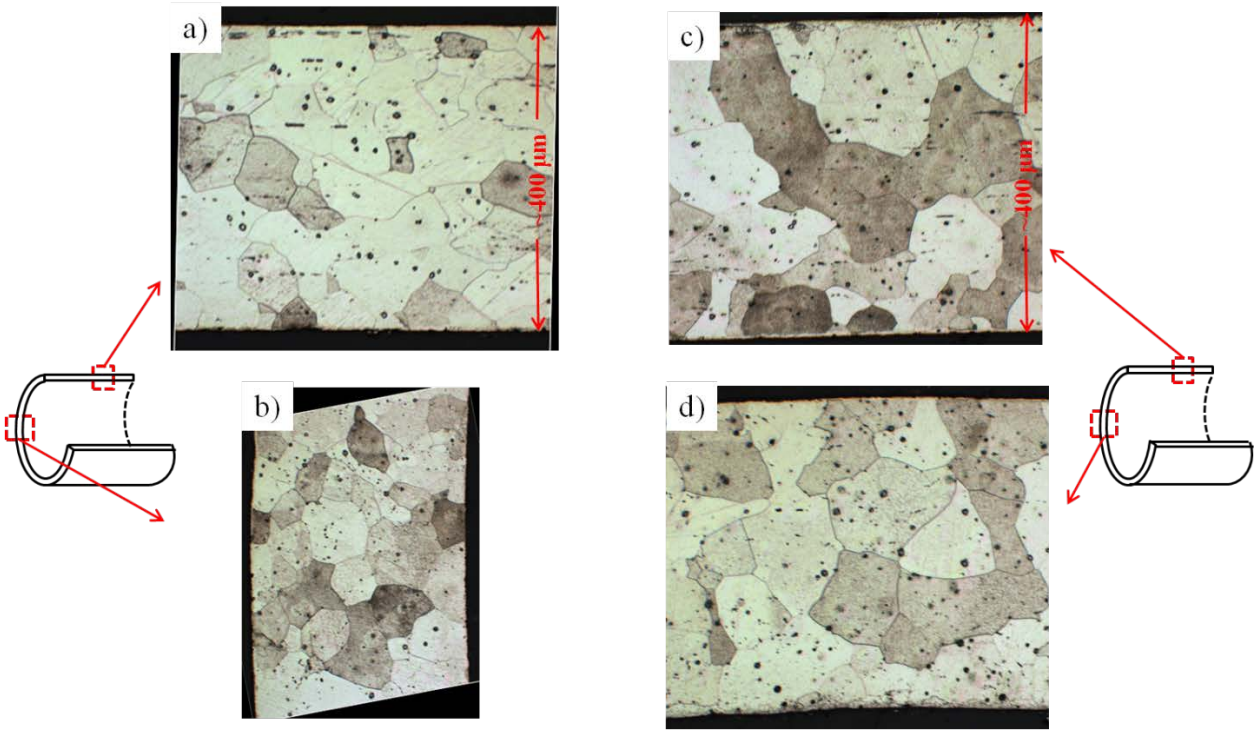

Figure 4: Optical micrographs of annealed samples at 850 C for 15 min after the last step of drawing; ORNL-A in a) cross-sectional direction b) longitudinal direction; ORNL-B c) cross-sectional direction d) longitudinal direction.

Crystallographic orientation distributions, degree of texture and strain introduced during deformation, grain size and misorientation angle distributions can be examined in detail by EBSD analyses. Figure 5 illustrates the crystal orientation maps of the ORNL A and ORNL-B as-drawn and annealed samples. The effect of annealing is very obvious since the as drawn samples (Figure 5.a and 5.c) have sub-boundaries as a result of deformation while annealed samples have strain free microstructure.

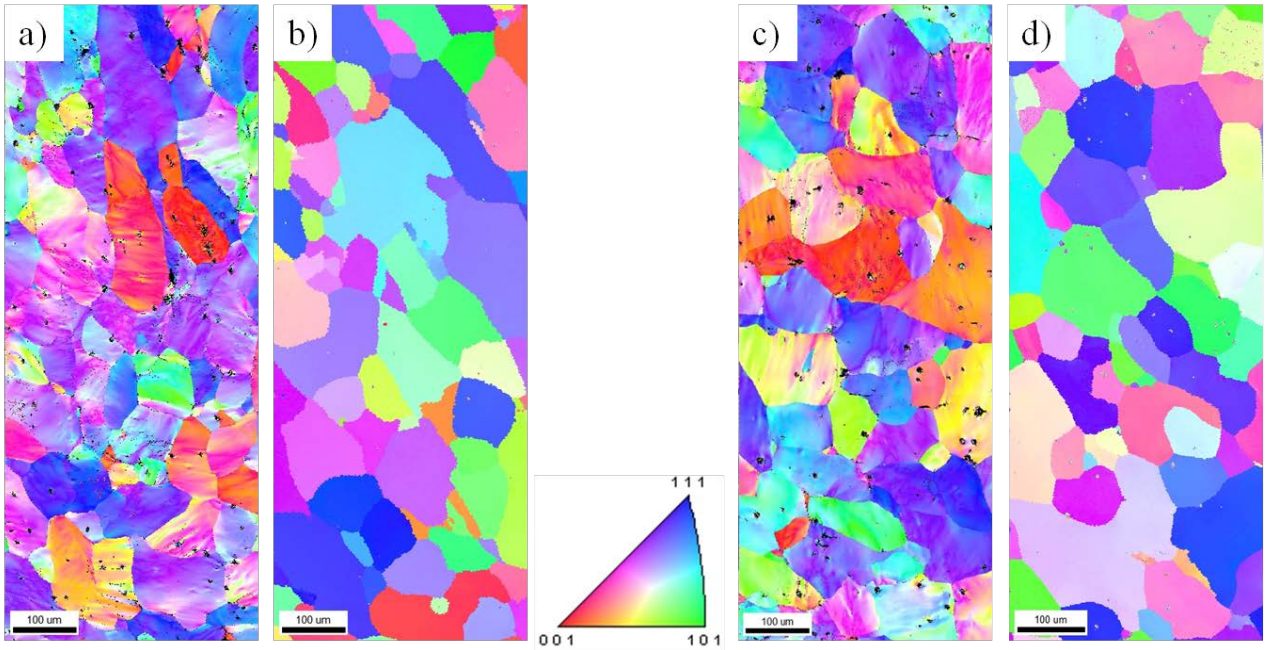

Figure 5: EBSD crystal orientation maps of ORNL-A a) as-drawn b) annealed at 850 °C for 15 minutes in hydrogen environment after the last drawing step; ORNL-B c) as-drawn d) annealed at 850 C for 15 minutes in hydrogen environment after the last drawing step.

Grain size distribution of as-drawn and annealed samples shows the same trend as well as very close average grain size values except ORNL-A as-extruded sample (Figure 6). The reason of such kind of difference might be attributed to the local statistics of the scanned area. It should be noted that while the grain size distribution follows a gaussian distribution after annealing, as-extruded samples show such a trend that the maximum number fraction is reached at the largest grain sizes. After annealing because of the recovery and growth by Ostwald ripening, there are small and large grains together (large grains will grow at the expanse of the small ones making large grains larger, small ones much smaller). On the other hand, during cold deformation, very large grains can be refined by the formation of subgrain boundaries as result of dislocation pile-ups. Consequently, there will be no very large grains nor were there very small grains since there is no growth or recrystallization.

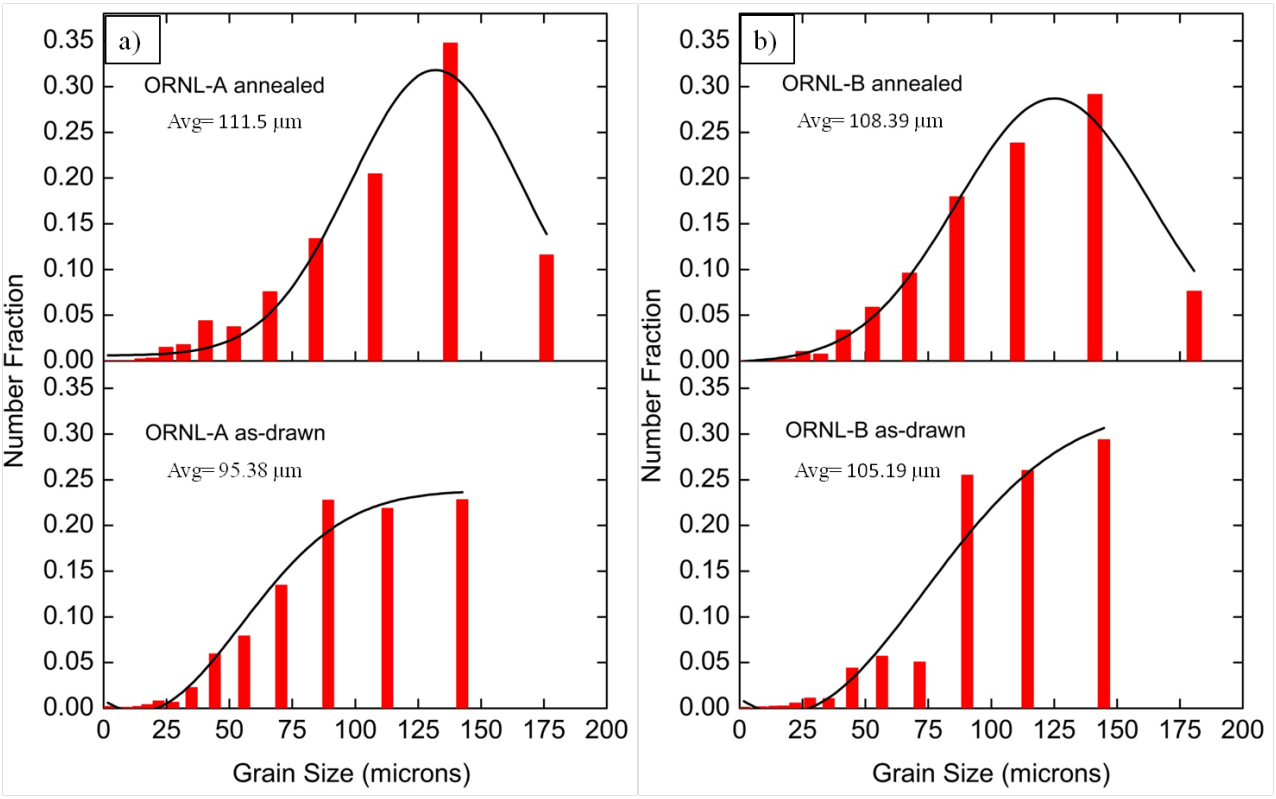

Figure 6: Grain size distribution of a) ORNL-A as-drawn and annealed samples b) ORNL-B as-drawn and annealed samples.

Figure 7 shows the misorientation angle distribution maps of ORNL-A and ORNL-B 'as drawn' and 'annealed' cases. In both types of first generation ORNL alloys, the amount of the low angle boundaries as a result of dislocation pile ups increases after the cold deformation (Figure 7.a&c). Figure 8 shows that almost 70% of the grain boundaries are the low angle grain boundaries with the misorientation angle <5°. On the other hand, annealing at 850 °C for 15 mins leads to the annihilation of dislocations and results in strain free microstructures (Figure 7.b&d). Annealing cleans the microstructure and results uniform distribution of misorintation angles as seen in Figure 8.

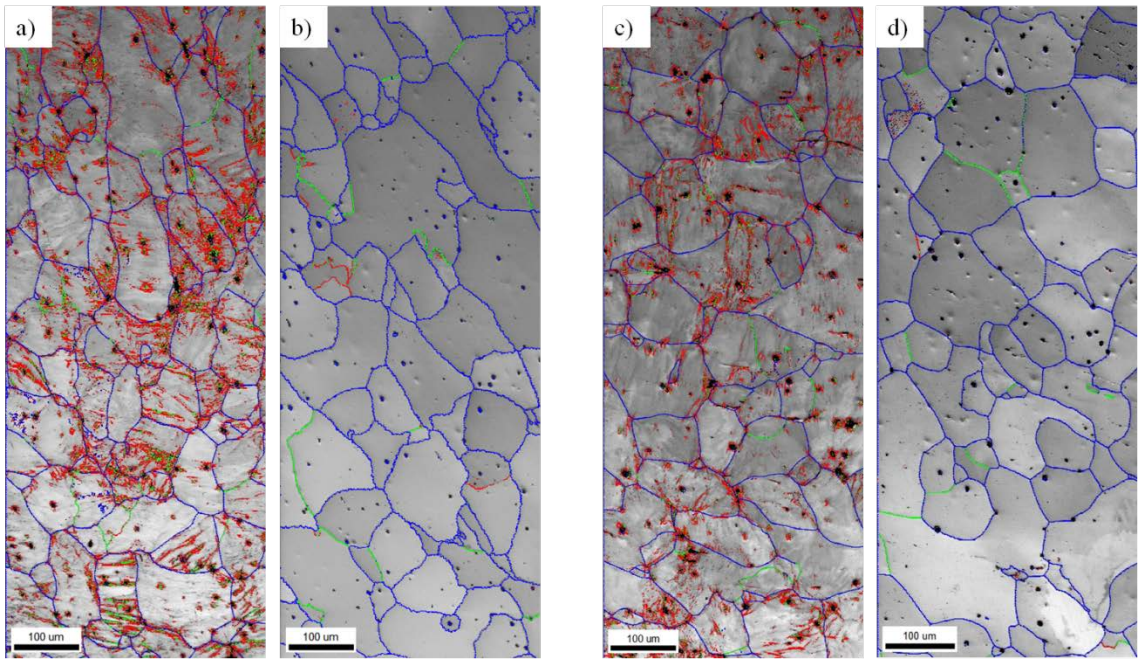

Figure 7: Rotation (misorientation) angle distribution map of ORNL-A a) as-drawn b) annealed samples; ORNL-B c) as-drawn d) annealed samples.

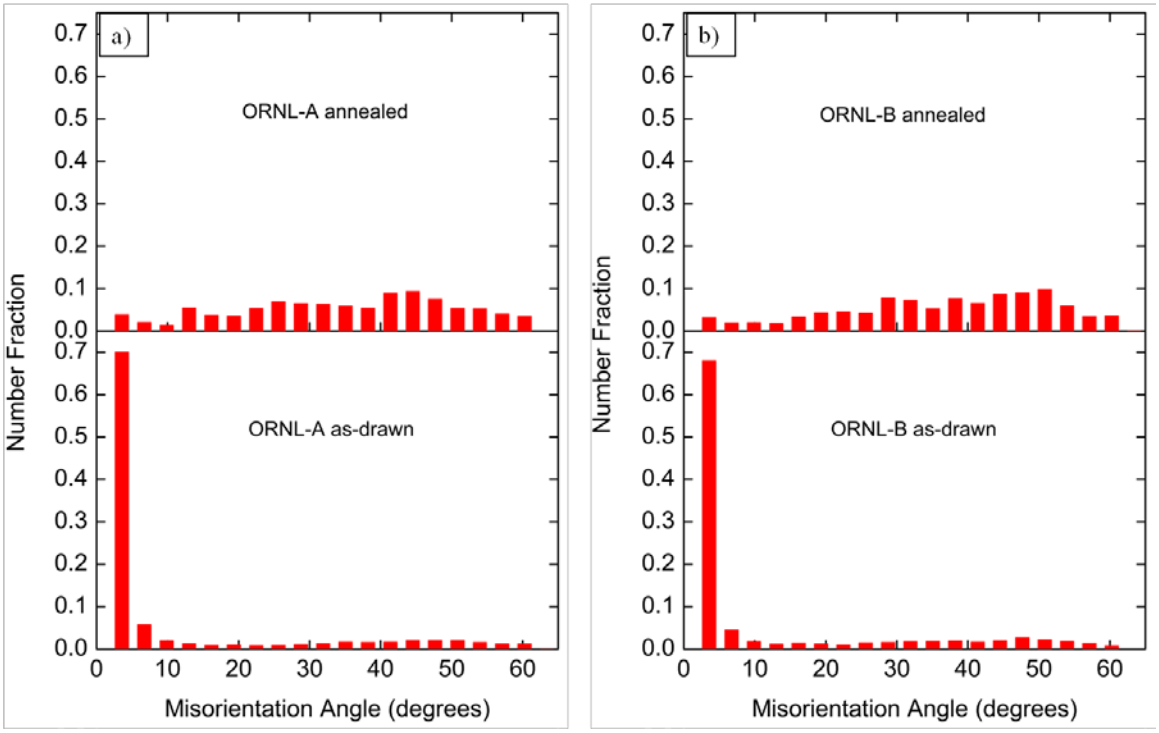

Figure 8: Grain size distribution of a) ORNL-A as-drawn and annealed samples b) ORNL-B as-drawn and annealed samples.

The local strain distribution of both first and second generation alloys was determined by using the kernel average misorientation (KAM) which is a local misorientation defined as an average misorientation of a point with all of its neighbors in a grain [4]. The KAM distributions represented by the color-coded maps in the ORNL-A and ORNL-B as-drawn and annealed alloys

are shown in Figure 9. As evidenced from the large number of low angle grain boundaries, cold working results in the residual strain in the alloys. The KAM maps in Figure 9.a&c indicate that the strain is concentrated along the grain boundaries rather than within the grain since the average misorientation angle increases at those regions. However, strain concentration around the large particles is more severe in both types of alloys due to the dislocation impingement by the second phase particles. On the other hand, KAM maps of annealed samples do not show any local strain concentration (Figure 9.b&d).

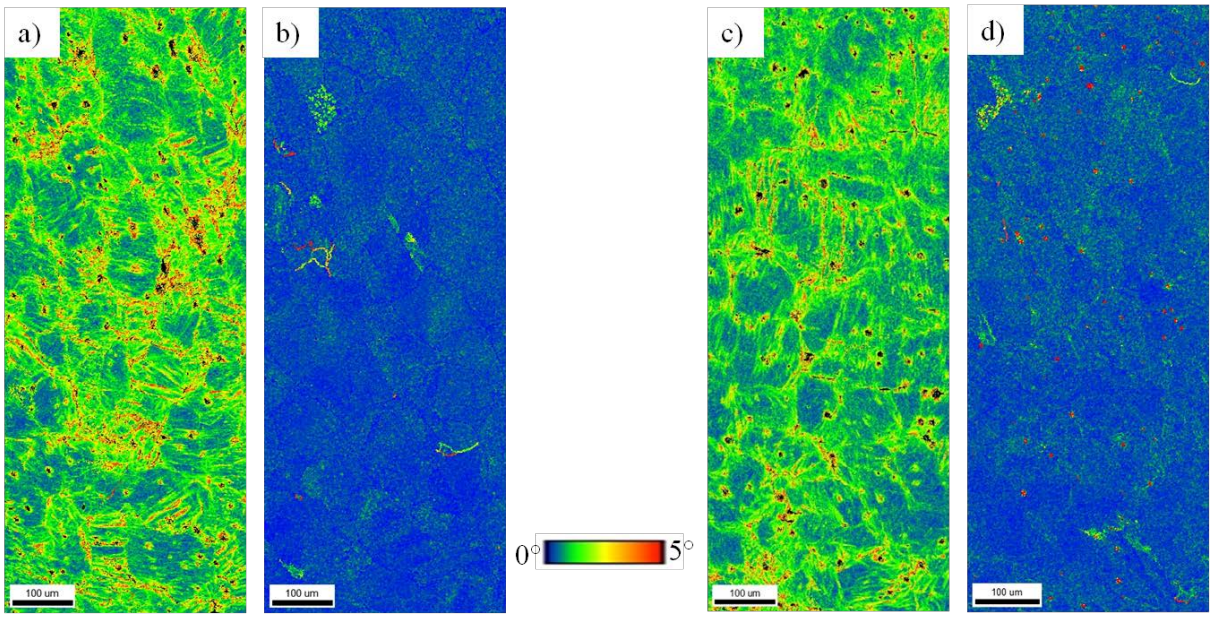

Figure 9: The color-coded mapping of kernel average misorientation in alloys ORNL-A a) as-drawn b) annealed samples; ORNL-B c) as-drawn d) annealed samples.

EBSD is a versatile method to explore the effect of deformation and annealing on texture. Figure 10 shows the {001} pole figures of first generation ORNL alloys. Since the samples were cut from the face of the tubes, the normal of (001) plane corresponds to the radial direction of the tubes. It can be inferred from Figure 10 that the grain orientation distribution is fairly uniform and there is no considerable change in the texture after deformation and annealing steps.

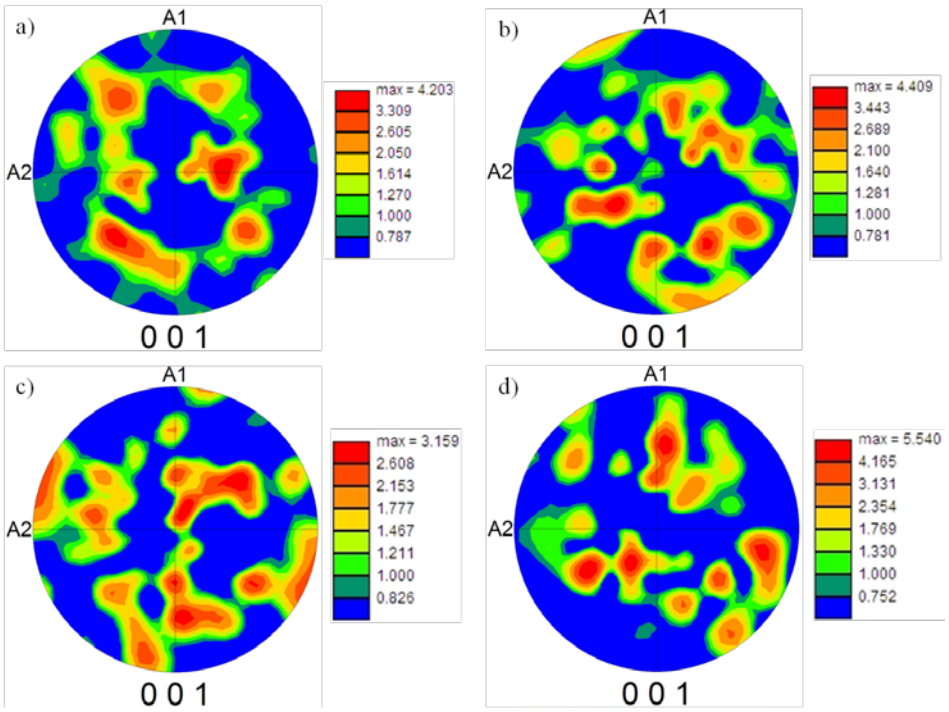

Figure 10: The {001} pole figures of ORNL-A a) as-drawn b) annealed alloys; ORNL-B c) as-drawn d) annealed alloys.

2nd generation ORNL Gen II alloy: Second generation alloys containing Nb and Mo are produced in a plate form. The microstructure is homogenous and grains are equiaxed (typical recrystallization microstructure) as shown in Figure 11.a. Image quality map in Figure 10.b shows that homogenously distributed second phase particles are elongated in the extrusion direction.

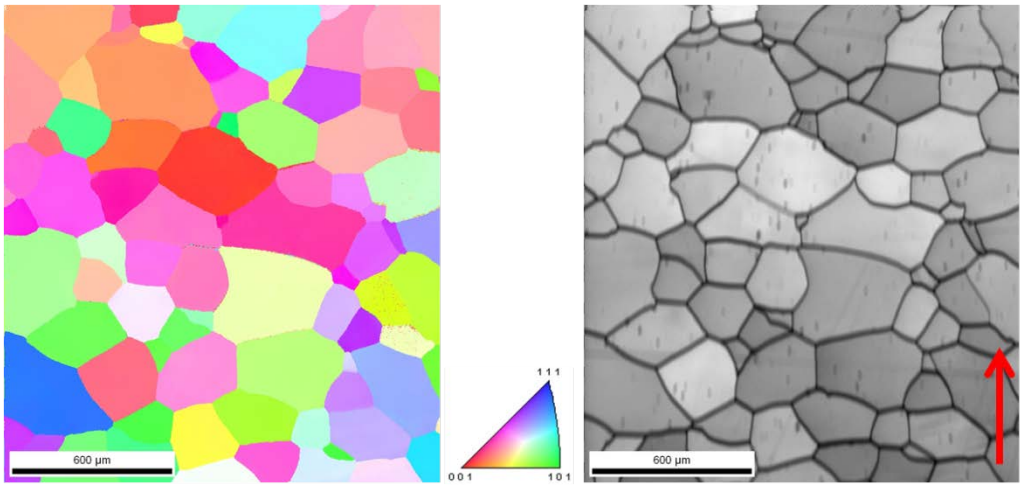

Figure 11: a) EBSD crystal orientation and b) image quality maps of Gen II FeCrAl alloy.

Figure 11 shows phase boundary map together with grain size and misorientation angle distribution plots. Since the minimum misorientation angle between the grains preset as 2°, the grain boundaries having lower misorientation angles will be missed. However, in Figure 12.a, although their misorientation angles are larger than 2°, four of the grain boundaries could not be

catched by TSL OIM Analysis program; therefore were not included into the grain size and misorientation angle calculations. Since the program cannot see those boundaries between two grains, it assumes a large single grain which in turn leads to increase in average grain size. In other words, the average grain size calculated as ~290µm in Figure 12.b should be lower. Moreover, although the misorientation angles between the grains seem to be concentrated around 30° and 60° as in Figure 12.c, the amount of the low angle grain boundaries would raise if those grain boundaries were also included.

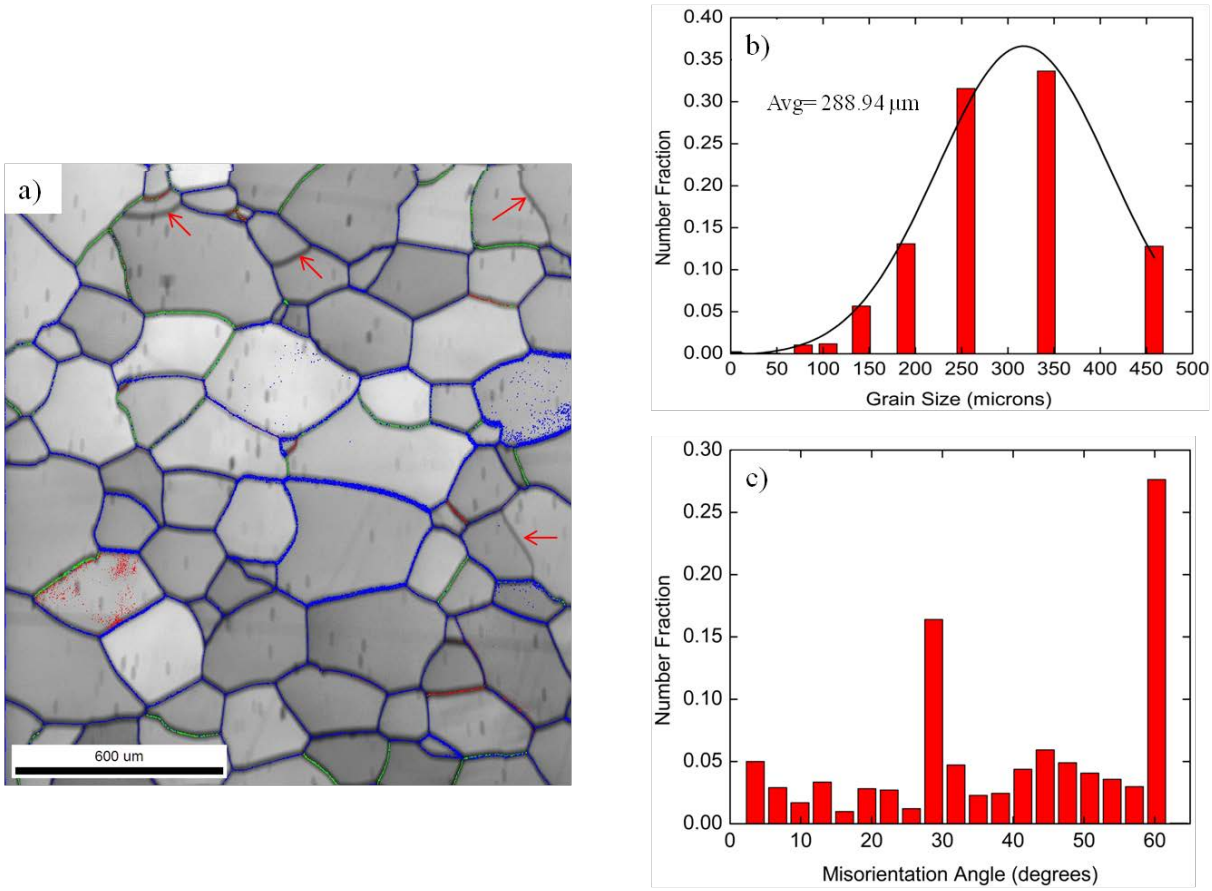

Figure 12: a) Phase boundary map (red arrows indicate the unidentified phase boundaries) b) grain size and c) misorientation angle distribution plots.

Similar to the first generation alloys, kernel average misorientation method has been utilized to determine the residual strains in the microstructure. Figure 13 indicates that the misorintation angle generally higher at the grain boundaries compared to inside of the grains. Contrary to the local strain around the large second phase particles in first generation alloys, smaller precipitates in Gen II alloy do not form strain field around.

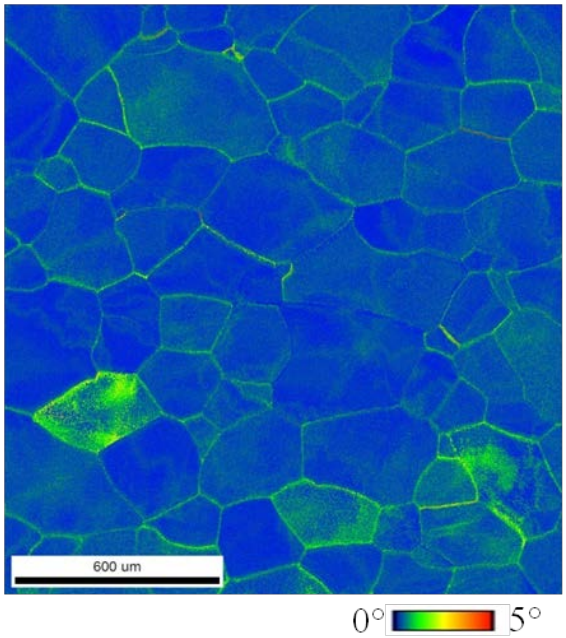

Figure 13: The color-coded mapping of kernel average misorientation in second generation ORNL Gen II alloy.

Figure 14 shows the {001} pole figures of second generation ORNL alloy. Since the sample was cut in such a way that the normal of (001) plane corresponds to the surface normal of the plate, A1 and A2 directions are the rolling and transverse directions, respectively. Although the microstructure indicates that the grain orientation distribution is fairly uniform, the texture index is a little bit higher than the tubular first generation ORNL alloys. If it is assumed that the difference is out of error, the reason can be attributed to the texture developed during hot extrusion. Even though the alloy is exposed to hot extrusion, during deformation second phase particles might precipitate along the grain boundaries restricting the boundary motion and leading to recrystallization in direction of deformation.

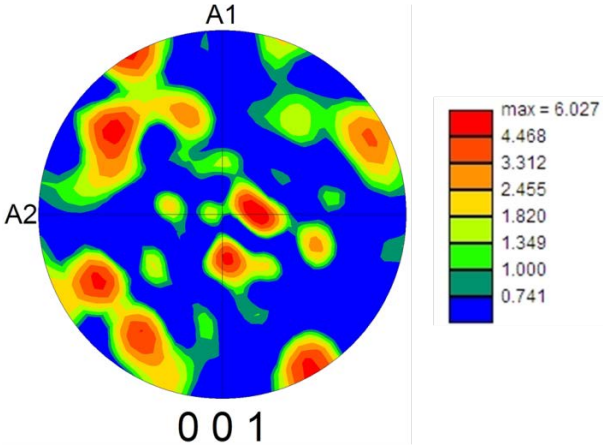

Figure 14: The {001} pole figure of ORNL Gen II alloy.

Summary

Microstructural analyses were performed on Gen I and II nuclear grade FeCrAl alloys developed at ORNL by using light optical microscopy together with electron back scattered diffraction. The highlights can be summarized as the following:

- Both first and second generation alloys show homogenous microstructures with homogenously distributed second phase particles. While the first generation ORNL-A and ORNL-B alloys contain large precipitates, second generation alloy has smaller second phase particles.
- While ‘annealed’ first generation and recrystallized Gen II alloys have the Gaussian grain size distribution as a result of recovery and recrystallization, ‘as-drawn’ first generation alloys show increasing grain size trend with a decreasing slope. It should be noted that the average grain size in Gen II alloy is larger than that of Gen I alloys.
- As a result of cold deformation, ‘as drawn’ first generation tubes show high density of low angle boundaries while annealed first and second generation alloys have relatively uniform misorientation angle distribution.
- Kernel average misorientation analyses indicate that the residual strain exists along grain boundaries and around large precipitates in ‘as extruded’ first generation alloys while ‘annealed’ alloys are almost strain free. On the other hand, second generation Gen II alloy has residual strain along grain boundaries not around the small precipitates.
- All of the alloy types at different conditions have uniformly distributed grains resulting in low texture values.

3.2 TENSILE TEST RESULTS

Engineering stress-strain curves obtained at room temperature (~27°C) are shown in Figure 3. Yield strength values were measured at 0.2% offset. The fitting parameters are not shown on the graph. ORNL A and B tubes show similar strength and elongation. Yield strength of Gen II is significantly higher than both tubes. However, Gen II fails right after yield in both tests.

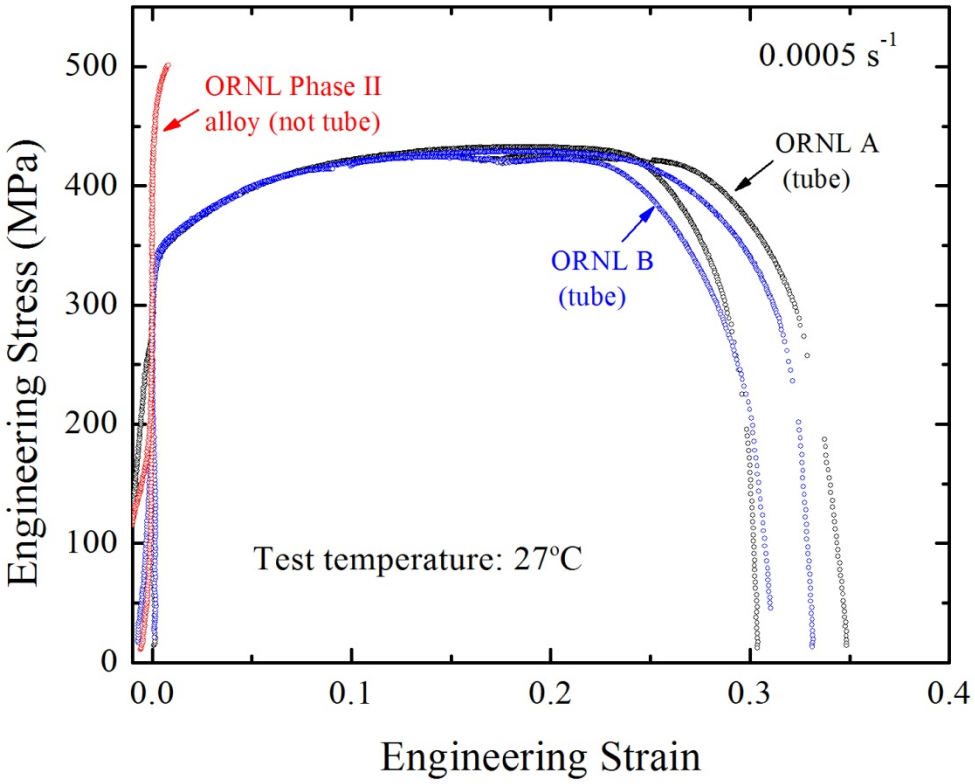

Figure 15. Engineering stress-strain curves of Gen I ORNL A and B tubes samples are shown together with Gen II (Phase II) alloy.
Both A and B tubes show 16-17% uniform elongation. The total elongation is more than 30% for both tubes.

High temperature testing

Engineering stress-strain curves obtained at 300 and 600°C are shown in Figures 16 and 17 respectively. At 300°C, while A show a little higher strength (yield and UTS), both tubes show similar uniform and total elongations as in room temperature testing. On the other hand, Gen II has higher strength and slightly lower elongation numbers than both tubes.

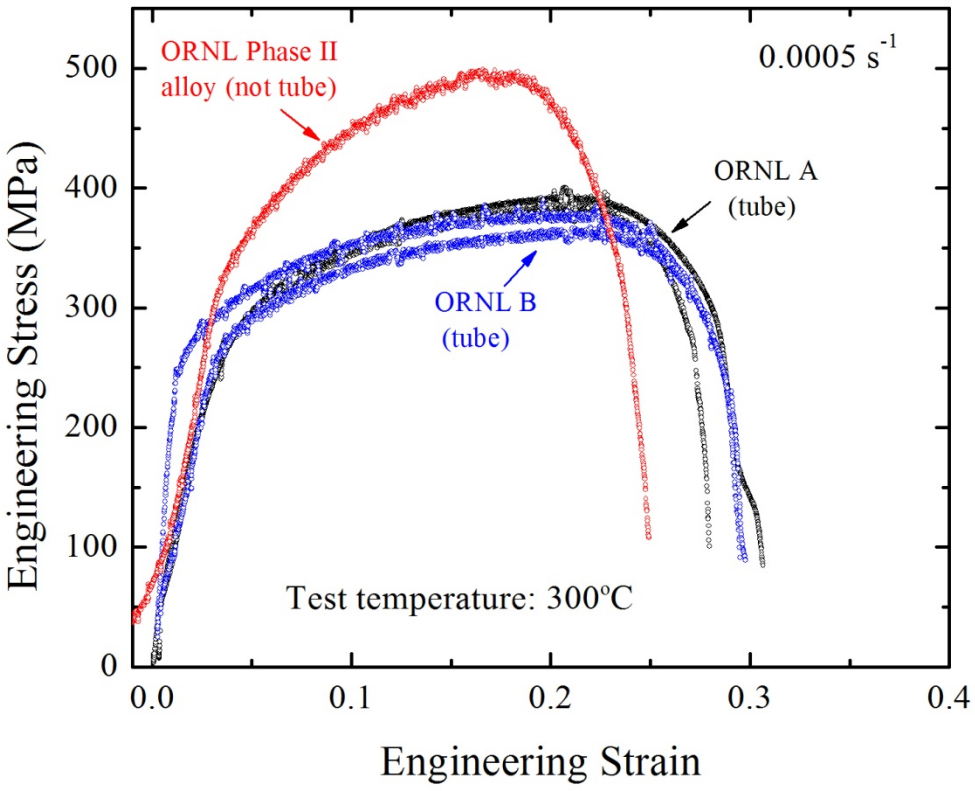

Figure 16. Engineering stress-strain curves of ORNL A&B tubes together with Gen II alloy tested at 300°C.

At 600°C testing shown in Fig. 17, Gen II shows significantly higher strength compared to tubes as in the case of 300°C and room temperature testing. Unlike previous cases, uniform elongation of Gen II is also better than both tubes while the total elongation is between the two tubes. Overall, except the room temperature testing of Gen II alloy, all the alloys show good mechanical properties as promising candidates for accident tolerant cladding applications. All the yield, UTS, and elongation results are tabulated in Table 2.

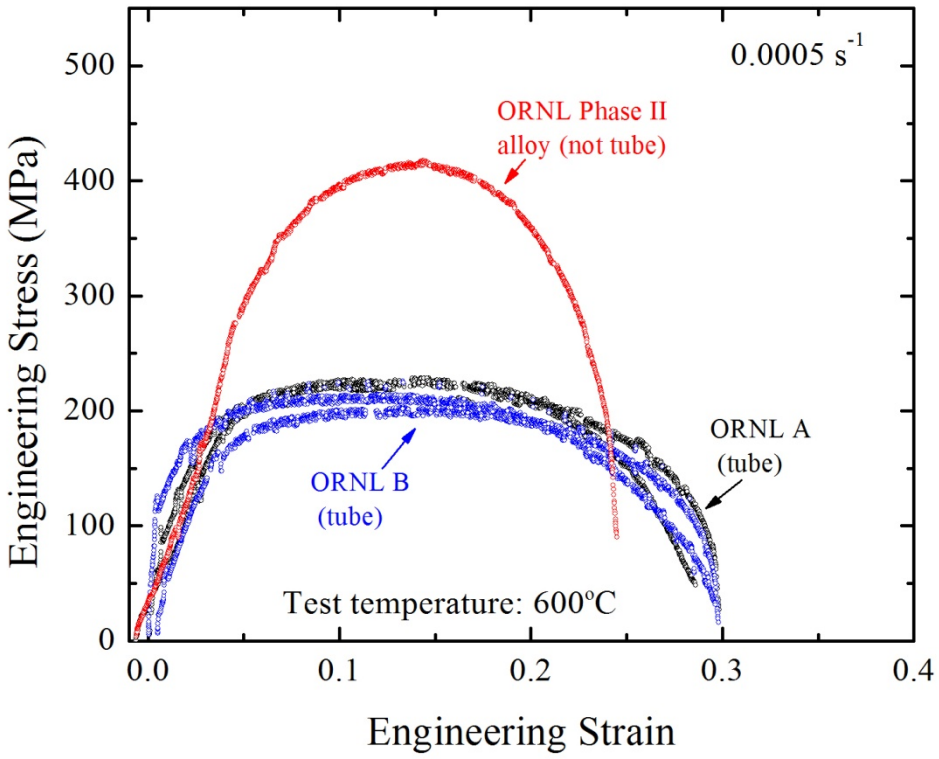

Figure 17. Engineering stress-strain curves of ORNL A and B alloys tested at 600°C.

Summary

Tensile testing was performed on Gen I and II nuclear grade FeCrAl alloys developed at ORNL at room temperature and elevated temperatures (300 and 600°C). Typical tensile behavior is observed for this class of alloys. The results are summarized in Table 2.

Table 2. Summary of the tensile tests on Gen I and II FeCrAl alloys at 23, 300, and 600°C.

23°C	σ_Y (MPa)	σ_{UTS} (MPa)	$\varepsilon_{uniform}$ (%)	ε_{total} (%)
ORNL A	360	429	17	32
ORNL B	355	426	16	31.6
Gen II	469	469	0.5	0.5
MA956	540	650		11
300°C				
ORNL A	285	388	20	28.5
ORNL B	257	369	20.5	29.5
Gen II	347	495	17	25
MA956	490	650	13	15
600°C				
ORNL A	198	224	12.5	29.5
ORNL B	142	205	12	22.5
Gen II	320	413	14	25
MA956	250	280	5	30

References

1. Engkvist, J., et al., *Alumina Scale Formation on a Powder Metallurgical FeCrAl Alloy (Kanthal APMT) at 900-1,100 A degrees C in Dry O-2 and in O-2 + H2O.* Oxidation of Metals, 2010. **73**(1-2): p. 233-253.
2. Terrani, K.A., S.J. Zinkle, and L.L. Snead, *Advanced oxidation-resistant iron-based alloys for LWR fuel cladding.* Journal of Nuclear Materials, (0).
3. Yamamoto, Y., *ORNL FeCrAl Alloy Development and Plate Processing for ATF Partners*, 2013, Oak Ridge National Laboratory.
4. Hou J., et al., *Effects of cold working degrees on grain boundary characters and strain concentration at grain boundaries in Alloy 600.* Corrosion Science, 2011 **53**(1137–1142).

4 MANUFACTURING PROCESS DEMONSTRATION FOR MA 956 ALLOY FUEL CLAD TUBING

4.2 Demonstration of Key Material Processing Steps

This report details progress in demonstrating the key material processing steps required for the manufacture of the candidate iron-based MA 956 alloy into nuclear fuel cladding tubes. The manufacturing process steps consist of the billet consolidation process, extrusion of the billet to a suitable rod or tube, and final forming of the extruded tube into a thin wall cladding tube using the tube pilgering process. In general, the pilgering process has two primary purposes, 1) pilgering can greatly improve the material grain structure, and 2) it is a way to reduce large amounts of the outside and inside diameter of a preexisting tube very quickly. The manufacturing process steps follow established cladding manufacturing processes used for materials such as the zirconium cladding alloys and titanium used in aircraft hydraulic tubing. A key difference with the MA 956 manufacturing process is that the starting alloy material is in the form of a mechanical-alloyed powder metal, which must be consolidated into a suitable bulk billet form. The following sections outline the manufacturing demonstration steps for the MA 956 cladding tube process.

4.2.1 Extrusion Billet Consolidation

The MA 956 alloy is produced as a Fe-based alloy by a high-energy mechanical alloying process. As such, the feedstock alloy is in the form of a fine metal powder having a heavily worked, fine grain microstructure that contains a small dispersion of oxygen. This powder metal feedstock must be consolidated into a highly dense metal billet that is suitable for hot extrusion using conventional direct extrusion press equipment. Figure 1 illustrates the key processing steps that will be demonstrated for the extrusion billet consolidation. The extrusion billet consolidation process consists of the following manufacturing steps:

- Preparation of the MA 956 metal powder using high-energy mechanical alloying of elemental powders
- Placement of the MA 956 powder into a thin steel can, cold compaction of the powder, and vacuum evacuation and sealing of the can
- Hot consolidation of the powder metal using Hot Isostatic Pressing (HIP) of the sealed can to achieve a 98+ dense billet suitable for the subsequent extrusion
- Removal of the can following the HIP process

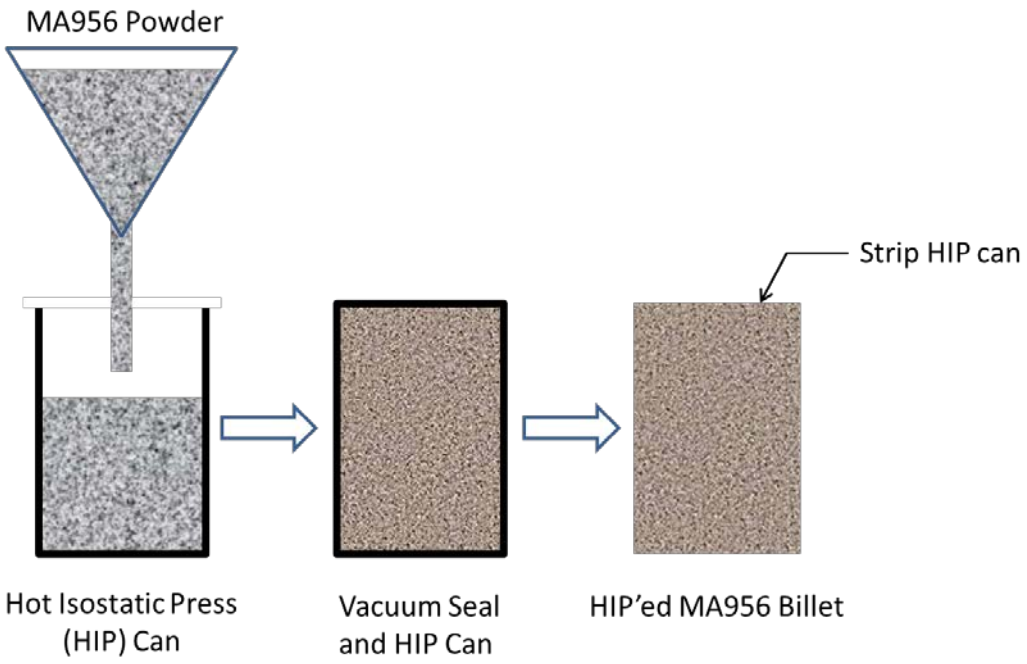

Figure 1. MA 956 Billet Consolidation

4.2.2 MA 956 Extrusion Manufacturing Step

To produce a raw tube shape suitable for the subsequent tube pilgering into the cladding tube dimensions, the consolidated MA 956 billet will be direct extruded to the form of a round rod or a tube through a conical extrusion die. A key objective of the extrusion processing step is to demonstrate the ability to extrude MA 956 at temperatures and extrusion forces that are compatible with commercial extrusion equipment. Figure 2 shows the direct extrusion process for production of an extruded tube. The relationship between the starting billet diameter and the final rod or tube outer diameters determine the extrusion ratio and amount of hot (elevated temperature) deformation that the material will undergo.

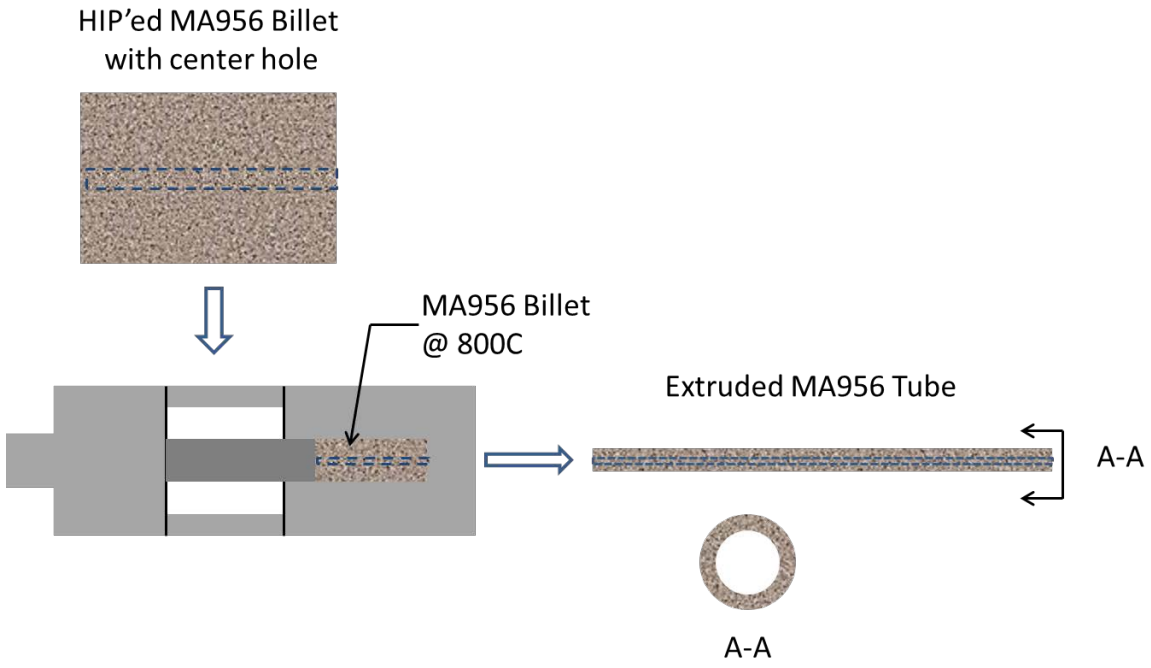

Figure 2. MA 956 Billet Extrusion to Tube

Because the MA 956 starts as a highly refined, fine grain microstructure that is stable at typical extrusion temperatures, achieving a high overall extrusion ratio is not necessary. This should result in a broader extrusion process window and lower required extrusion forces.

4.2.3 MA 956 Tube Pilgering Manufacturing Step

The final step in producing the MA 956 cladding tube is the demonstration of tube pilgering to form the rough extruded MA 956 tube into the final thin wall cladding tube form. Pilgering is an established tube forming process that combines deformation modes in a unique process. It has been used extensively to produce zirconium alloy cladding and industrial tubing and for high pressure titanium hydraulic tubing. Pilgering can produce high levels of cold deformation in hard to process materials, as well as produce advantageous textures in the material. The basic pilgering process that will be demonstrated for the MA 956 tube cladding is illustrated in Figure 3. A critical element of the overall manufacturing process demonstration is to show that a high quality MA 956 tube can be extruded to dimensions that are suitable for the starting point of the pilgering process. The tube pilgering process demonstration will be conducted by an established commercial tubing manufacturer, Sandvik Special Metals.

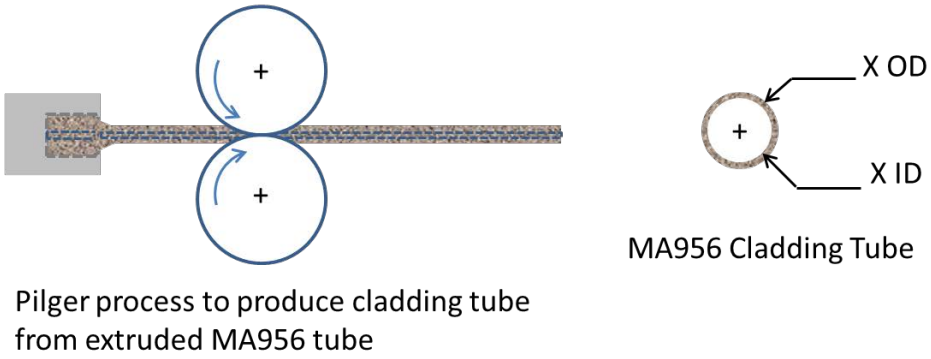

Figure 3. MA 956 Pilger to Thin Wall Cladding

4.3 MA 956 Manufacturing Process Demonstration Results

1.1.1.1

4.3.1 Billet Consolidation and Fabrication

The processing of MA 956 mechanical-alloyed (MA) powder into a solid metal billet required canning of the powder in a mild steel can followed by elevated temperature and pressure hot isostatic pressing. PNNL provided approximately 5 kg of MA 956 powder to BodyCote (Andover, MD) for HIP consolidation into a solid billet having 1.75 inch diameter and 20 inch length after removal of the steel HIP can. HIP parameters used by BodyCote were a temperature of 1065 °C for 240 minutes and a pressure of 14,750 psi. While the HIP process requires an extended dwell time at pressure and temperature, it has been shown to be economically viable for the consolidation of many different metal alloys for a wide range of commercial applications.

Following delivery of the HIP-consolidated MA 956 billet, individual extrusion billets were machined from the larger rod. The extrusion billets were sized to fit inside a high purity copper outer can. During the extrusion process, the copper can acts as a metal lubricant between the extrusion die and the MA 956 billet, improving overall surface finish and providing protection for the die surface. Combined with a high

temperature grease-type lubricant, this approach has been used successfully to extrude a number of high temperature alloys using the PNNL benchtop extrusion press. Figure 4 shows a picture of a typical MA 956 extrusion billet assembly with the MA 956 solid billet and the copper outer can and end lid prior to and after assembly.

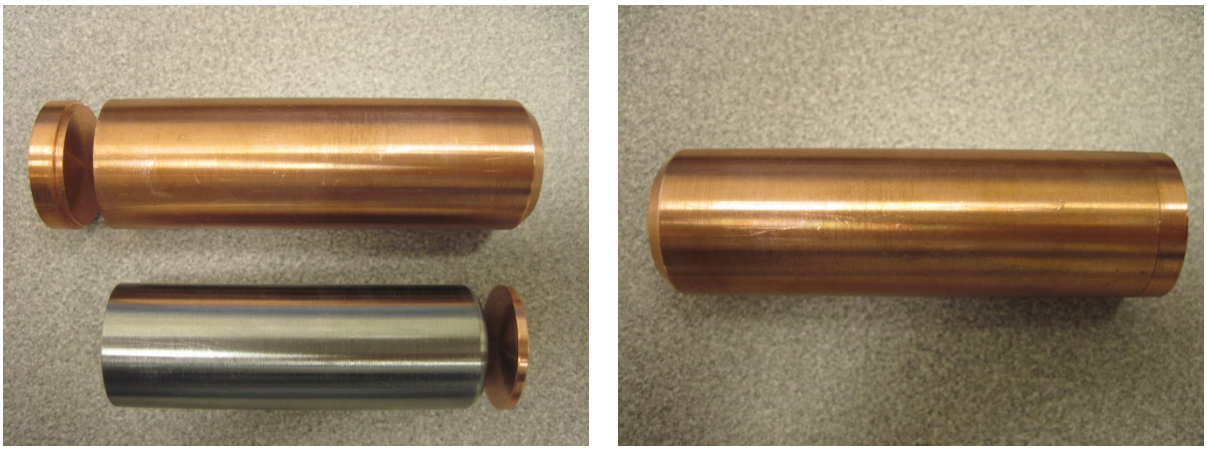

Figure 4. MA 956 Billet Assembly

1.1.1.2

4.3.2 MA 956 Extrusion Process Development and Demonstration

The MA 956 material is an iron-based high temperature alloy produced by a mechanical alloying process involving high energy ball milling of Fe and alloying elements. The MA process introduces a certain percentage of distributed oxygen into the resulting powder which improves elevated temperature strength and properties. At the same time, the oxygen and alloy composition of MA 956 result in relatively high strength at elevated temperatures, which in turn, requires higher extrusion forces. During the extrusion development and demonstration phase, a number of technical challenges were encountered. The elevated temperature flow stress of MA 956 required that the extrusion be run at the highest possible temperature in order to reduce the flow stress and thus the maximum extrusion force or tonnage. With the use of a high purity copper outer can, the maximum billet temperature was established at 1000 °C, which is slightly below the melting temperature of copper. However, the temperature of the extrusion tooling used with the PNNL press is limited to a maximum of 350 to 400 °C in order to retain the strength of the H-13 and H-21 steel tooling. The high temperature of the MA 956 extrusion billet (1000 °C) and the relatively cool tooling result in the potential for significant cooling of the billet during the transfer from the pre-heat furnace, loading of the billet into the container and initiation of the actual extrusion. As a result, significant efforts were focused on minimizing transfer and extrusion time in an effort to prevent excessive cooling of the MA 956 billet prior to extrusion.

The billet cooling issue is somewhat specific to the PNNL benchtop extrusion system. In commercial practice, extrusion presses have large diameter containers that allow extrusion of large diameter billets, usually in the range of 6 to 18 inch diameter. In this case the extrusion billet has relatively high thermal mass, and although the outer surface of the billet can undergo cooling during transfer and initiation of the

extrusion, the majority of the billet remains at or near the target billet temperature. In the case of the PNNL extrusion press, the thermal mass of the extrusion billet is quite small due to the small billet diameter and length and it is loaded into a comparatively large container that is at a significantly lower temperature. This results in the potential for significant cooling of the MA 956 billet material with a corresponding increase in the flow stress of the material as temperature drops from the target 1000 °C. Initial attempts to extrude MA 956 directly to a tube (using an internal floating mandrel) at 10:1 ratio resulted in stalling of the extrusion press at its maximum extrusion force. Extrusion directly to a tube form typically requires a higher overall extrusion ratio, and more significantly has higher friction and the potential for greater cooling of the billet, particularly for the small billets required for the PNNL extrusion press. Due to these limitations, subsequent MA 956 extrusion development focused on extrusion of solid rod using a moderate extrusion ratio.

Two MA 956 extruded rods at a 4:1 ratio were successfully processed during the extrusion phase of the MA 956 manufacturing demonstration. Using a copper canned billet rod lengths of approximately 8” inches were produced. Following extrusion the MA 956 rods were etched in nitric acid to remove the copper can cladding and heat treated at 1000^{o}C for 1 hr in vacuum to off-gas any hydrogen absorbed during etch and produce a uniform microstructure. After improvements to the billet transfer was made by installing an autoloader and extrusion speed was increased by changing a valve body a tube reduction at 6:1 was made in the MA956 and is shown here in Figure 5. The force required for the 6:1 tube extrusion indicated that even higher ratios or lower temperatures are possible. The rod extrusions were processed to tubes for pilgering. Figure 6 shows a photograph of the extruded MA 956 rods after removal of the outer copper can.

Figure 5. Photograph of the MA 956 Tube Extrusion

Figure 6. Photograph of the Cleaned and Etched MA 956 Rod Extrusions

In order to produce a tube blank with dimensions from the rods suitable for the final pilger tube process, both MA 956 rods were supplied to Tube Hollows (Dearborn, MI) for straightening and boring of the center hole. Tube Hollows specializes in processing long, thin wall tubes from a wide range of materials using specialized proprietary processing methods. Figure 7 shows a view of the finished MA 956 tube blanks after processing by Tube Hollows, and prior to delivery to Sandvik for the final pilger processing into cladding tube samples.

Figure 7. View of MA 956 Tube Blanks after Processing by Tube Hollows.

The final process demonstration step for fabrication of MA 956 cladding tube will be the application of the tube pilgering process by Sandvik Special Metals. Sandvik is an international producer of tube products for nuclear fuel cladding and high pressure hydraulic tubing. A key fabrication technology developed by Sandvik is the use of the tube pilgering process for reducing a relatively thick wall tube to the required thin wall tube dimensions specified for fuel cladding and hydraulic tubing. In addition to being an efficient process for making large cold reductions in tube outer and inner diameters, pilgering can also be used to impart favorable crystallographic textures in many difficult to process metals, such as zirconium and titanium. The ability to make large reductions and generate favorable textures in hard to process materials has established tube pilgering as the most economical fabrication method for production of nuclear fuel cladding.

5 MA 956 MANUFACTURING CONCLUSIONS

PNNL has developed the manufacturing and processing steps for consolidating MA-956 metal powders into billet form, hot extruding from billet to rod or tube. The next steps are to subsequently cold form the tube into cladding tube dimensions through the application of the tube pilgering process.

6 SUMMARY AND PATH FORWARD

Research on tube processing on FeCrAl alloys shows a viable path forward for producing long thin walled tubing for production of the Gen I and Gen II FeCrAl alloys (with Mo added). Although tubing was made on the Gen II FeCrAl alloy with Mo added, more research is needed to obtain longer tubing with a uniform wall thickness. Attempts to produce tubing from the Gen II FeCrAl alloy with Mo and Nb added were not successful at Century tubing or at Rhenium Corporation. Progress was made towards making tubing from MA-956 at PNNL through reductions performed with hot extrusion at 1000C. This has provided initial thick walled tubes to be used for tube pilgering at Sandvik. Future work will center on testing on long tubing from Gen I FeCrAl alloy, further developments to improve the final drawn Gen II FeCrAl tubing with Mo and pilger testing on MA-956.

7 REFERENCES

1. Dr.-Ing. Laue, Kurt (Formerly Director of Vereingte Deutsche Metallwerke, Frankfurt) & Dr.-Ing. Stemger, Helmut (Technical Director of Glyco do Brasil Industria Metallurgica, Ltda. Cataguases, Brazil, “Extrusion” (copyright in English), Published in US by American Society for Metals, (1981).

2. Bennett, W.D., Doherty A. L., Geelhood K. J., Henager, Jr., C.H., Lavender C. A., Love, D.L., Omberg R. P. and Smith, M.T., “FY-15 Technology Implementation Plan for the U-Mo Fuel Concept” Pacific Northwest National Laboratory, PNNL-24078, FCRD-FUEL-2015-000453, (February 2015).